Chemistry and Physics of Lipids 224 (2019) 104707

Contents lists available at ScienceDirect

Chemistry and Physics of Lipids

journal homepage: www.elsevier.com/locate/chemphyslip

Cabazitaxel and thymoquinone co-loaded lipospheres as a synergistic combination for breast cancer

Nagavendra Kommineni, Raju Saka, Upendra Bulbake, Wahid Khan*

Department of Pharmaceutics, National Institute of Pharmaceutical Education & Research (NIPER), Hyderabad, 500037, India

ARTICLE INFO

Keywords:
Cabazitaxel
Thymoquinone
Lipospheres
Breast cancer
Synergistic combination

ABSTRACT

Cabazitaxel as microtubule inhibitor and thymoquinone as HDAC inhibitor affects the important genes like p53, STAT3, Bax, BCL-2, p21 and down regulation of NF-κB are reported for potential activity against breast tumors. However, poor aqueous solubility and permeability hinders the delivery of these drugs to target site. To address the delivery challenges cabazitaxel and thymoquinone co-loaded lipospheres were developed. Lipospheres are the lipid based self-assemblies of particle size below 150 nm were prepared with more than 90% entrapment efficiency for both the drugs. *In vitro* drug release studies revealed there was a sustained diffusion controlled drug release from liposphere matrix leading to decrease in particle size with increase in zeta potential. Cytotoxicity studies on MCF-7 and MDA-MB-231 cells demonstrated cabazitaxel and thymoquinone as synergistic combination for the treatment of breast cancer which was proved by CompuSyn software. Enhanced efficacy of developed lipospheres can be due to rapid cellular internalization which was observed in confocal laser scanning microscopy. Drastic changes in cancer cell morphology such as nuclear fragmentation were observed upon treatment with these lipospheres in comparison to combination solution as observed in fluorescent imaging which are the hall marks of apoptosis. Cell cycle analysis and apoptosis studies confirmed the increased Sub G1 phase arrest as well as cell death due to apoptosis. Thus, as per observed results, it can be concluded that cabazitaxel and thymoquinone co-loaded lipospheres are the efficient delivery vehicles in management of breast cancer.

1. Introduction

Breast carcinoma is the leading cause of death in women in most of the developed countries (Stewart and Wild, 2017). The treatment remedies depend on the stage of the developed carcinoma. At early stages surgery is performed in combination with chemotherapy followed by radiation therapy. Late stages of breast carcinoma are difficult to cure and the life span of the patient will decline. Much of the chemotherapy is associated with poor absorption, penetration into tumor tissues which may lead to low therapeutic benefit, severe side effects and death in some cases (Miller et al., 2016). Combination therapy was emerged to improve the patient life expectancy by acting in either synergistic or additive manner or by reducing the side effects of the other chemotherapeutic (Pratt et al., 1994). However, lack of tumor targeting, toxicity to normal cells were the major drawbacks for available drugs. To overcome this situation, targeting the chemotherapeutics to disease site especially in case of carcinoma has been explored extensively nowadays (Ma et al., 2013).

Taxanes are the most promising microtubule inhibitors to eradicate several types of tumors (Jordan and Wilson, 2004). Drug resistance is the major hurdle which needs adjuvant therapy to suppress the disease progression and also to reduce the drug related side effects (Kitano, 2004). For reducing the resistance in monotherapy and to eradicate tumors, two or more chemotherapeutics are needed which will act by either synergistic or additive mechanism (Al-Lazikani et al., 2012). Cabazitaxel (CBZ) has been approved for hormone refractory prostate cancer. Jevtana® is the micellar CBZ solution with severe side effects like neutropenia, anaemia, thrombocytopenia, diarrhoea and

Abbrevations: CBZ, cabazitaxel; TMQ, thymoquinone; LSP, lipospheres; sol, solution; DMEM, Dulbecco's Modified Eagle's Medium; FBS, fetal bovine serum; RP-HPLC, reverse phase high performance liquid chromatography; PDA, detector Photo dynamic array detector; PDI, poly dispersity index; PBS, phosphate buffer saline; DMSO, dimethyl sulfoxide; MTT, 3-(4, 5- dimethylthiazol-2-yl)-2, 5-diphenyltetrazolium bromide; TO, triolein; TP, tripalmitin; TM, trimyristin; NMP, N-methyl-pyrrolidone; TC, tricaprin; TS, tristearin; kDa, kilodaltons; mL, milliLiter; Egg PC, egg phosphatidyl choline; DL, drug Loading; AO, acridine orange; EtBr, ethidium bromide; PI, propidium Iodide; FITC, fluorescein isothiocyanate; EPR, enhanced permeation and retention; EE, entrapment efficiency; Fig, figure

* Corresponding author.
E-mail address: mail4wahid@gmail.com (W. Khan).

https://doi.org/10.1016/j.chemphyslip.2018.11.009
Received 18 May 2018; Received in revised form 19 September 2018; Accepted 29 November 2018
Available online 04 December 2018
0009-3084/

neutropenic fever which leads to death limits its clinical use (Reddy and Bazile, 2014; Lydon, 2011). Recently CBZ has been reported for its activity in HER-2 negative breast cancer (Kümmel et al., 2017). Developing formulation for this drug is a challenging task as it possess poor aqueous solubility and permeability (Mahajan et al., 2015).

Thymoquinone (TMQ) is a phytochemical compound which has been extracted from the seeds of *Nigella sativa*/Black seed/Black cumin. TMQ exhibits anti-tumor activity against breast cancer (Pratama, 2017), ovarian cancer, lung cancer, colon cancer as well as in leukemia (Gali-Muhtasib et al., 2006; Khan et al., 2017). There are reports available that TMQ act as an angiogenesis inhibitor as well as an HDAC inhibitor, that it affects the important genes like p53, STAT3, Bax, BCL-2, p21 and cause down regulation of NF-κB (Kodappully Sivaraman Siveen et al., 2014; Rahmani et al., 2014) and also acts as better adjuvant therapy for cancer treatment (Mostofa et al., 2017). TMQ is a sensitive molecule which degrades in presence of light, heat, pH and also it has poor aqueous solubility which are the major drawbacks (Lebwohl and Ali, 2001; Salmani et al., 2014). Developing formulation for TMQ is a difficult task which can be overcome by loading in lipid based formulations.

Nanocarrier mediated delivery of chemotherapeutic agents with size less than 200 nm targets the tumor site either by passive manner (Enhanced permeation and retention (EPR) effect) or by active targeting (Surface functionalized nanocarriers with ligands/ aptamers/ antibodies). Biodegradable polymers and lipids are extensively used to deliver the drugs to targeted site (Muntimadugu et al., 2017; Peer et al., 2007). Lipids play a vital role in enhancing permeability through biological membranes of cells and tissues. Lipospheres (LSP) are the lipid based self-assembled systems containing solid hydrophobic lipid core surrounded by a layer of phospholipid molecules. LSP have several advantages over other lipid based systems such as low cost of reagents, ease of manufacturing, rapid dispersibility in an aqueous medium with controlled drug release rate. Cyclosporine loaded LSP (Deximune® soft-gelatin capsules Dexcel Pharma Ltd.) were in clinical use with enhanced oral bioavailability (Bekerman et al., 2004; Avramoff et al., 2012). LSP have been explored for topical delivery of chemotherapeutics (Avramoff et al., 2012; Jain et al., 2017, 2016) as they have capability to permeate the cells and tissues. But, very less reports were available to deliver these carriers loaded with drugs through parenteral administration (Elgart et al., 2012). In this study we investigated delivery of two drugs in LSP as a co-loaded nanocarrier for effective management of breast carcinoma synergistically with enhanced cellular permeation and cell death due to apoptosis.

2. Materials and methods

2.1. Materials

CBZ obtained as a gift sample from TherDose Pharma Pvt. Ltd. (Hyderabad, India), Triolein (TO), Tripalmitin (TP), Trimyristin (TM) and N-methylpyrrolidone (NMP) were purchased from HiMedia Laboratories (Mumbai, India). Tricaprin (TC) and Tristearin (TS) were purchased from TCI chemicals Pvt. Ltd. (Tokyo, Japan). Thymoquinone, Egg phosphatidyl choline, Vitamin E-TPGS, Fluorescein isothiocyanate (FITC), Acridine orange, Ethidium bromide, Rhodamine, 3-(4, 5- dimethylthiazol-2-yl)-2, 5-diphenyltetrazolium bromide (MTT), trypsin-EDTA and cellulose dialysis tubing with 12,000 Da molecular weight cut off, fetal bovine serum (FBS), L-glutamine, antibiotic solutions, Acridine orange, Ethidium bromide were purchased from Sigma Aldrich (St. Louis, MO, USA). Ethanol was purchased from Jiangsu Huaxi International Trade Co.Ltd (China), the cell culture media and supplements including Dulbecco's Modified Eagle's Medium-high glucose (DMEM) was purchased from HyClone, GE Health Care Life Sciences, Logan, UT. Amicon ultra 10 kDa cut off centrifugal filters were purchased from Merck Milpore (Germany). Acetonitrile (MeCN) was purchased from Merck Specialities Pvt. Ltd. (Mumbai, India). All other ingredients and reagents were of analytical grade.

2.2. Methods

2.2.1. Analytical method

An isocratic RP-HPLC (Waters, USA) method for simultaneous quantification of CBZ and TMQ was developed. A series of standard solutions were prepared in concentration range of 0.25 to 32 µg/mL from methanolic solutions of CBZ and TMQ (1 mg/mL). Acetonitrile: 0.1% v/v formic acid (60: 40 v/v) was used as mobile phase. Analysis was carried out using a reversed phase InertSustain C18 column (150 × 4.6 mm, 3.5 µm particle size) at flow rate of 1 mL/min, 20 µL injection volume, 230 nm for CBZ and 254 nm for TMQ as detection wavelengths.

2.2.2. Preparation and optimization of CBZ TMQ co-loaded LSP

CBZ TMQ co-loaded LSP were prepared by melt dispersion method as per earlier reports with slight modification (Jain et al., 2016). Selection of drugs and their solubility in type of solvent, solubility of drug in type of core lipid, core lipid: coat lipid ratio and core lipid: surfactant ratios are the critical parameters for controlling size of LSP. Different parameters were optimized for co-loaded LSP preparation including type of core lipid, type of solvent, % DL whereas core lipid to coat lipid ratio and combination of stabilizers with ratio were kept constant and different formulations were prepared. For optimization of formulations, egg phosphatidyl choline (Egg PC-20 mg) was dissolved in appropriate quantity of ethanol and maintained at 50 °C. Simultaneously, TC/TM/TS/TO/TP (40 mg), T80 (20 mg)and Vitamin E-TPGS (40 mg) were melted at 50 °C and added to the Egg PC solution with continuous stirring at 500 rpm to form blank preconcentrate. CBZ, TMQ were dissolved in ethanol (100 µL) and were added to the above preconcentrate followed by vortexing for 10 min at room temperature to achieve drug loading. CBZ TMQ co-loaded preconcentrate was stored at 2–8 °C and reconstituted with millipore water at 37 °C before use to get CBZ TMQ co-loaded LSP.

2.3. Characterization of CBZ TMQ co-loaded LSP

2.3.1. Particle size distribution

Mean particle size (z-average) and polydispersity index of CBZ TMQ co-loaded LSP were measured using Malvern Zetasizer Nano (Malvern Instrument Ltd., Malvern, UK) at 25 °C using 90° scattering angle in triplicate. Particle size distribution for optimized final formulation was performed as intra-day and inter-day to check the reproducibility.

2.3.2. Surface morphology

Transmission electron microscopy (TEM) was used to determine the morphology of CBZ TMQ co-loaded LSP. Briefly, CBZ TMQ co-loaded LSP were deposited on formvar® copper grids and stained using 2% uranyl acetate at 25 ± 2 °C. Images were recorded with JEM 2100 transmission electron microscope (JOEL, Japan) using Gatan digital micrograph software. Sample was loaded on grids with carbon tape and gold coating was performed for 120 s. Images were recorded using scanning electron microscope (Quanta 250, FEI,USA) in high vacuum mode at a voltage of 5 kV.

2.3.3. Drug loading and entrapment efficiency

Theoretical drug loading was varied from 1.5 to 5.5 % w/w for each drug in LSP. CBZ and TMQ entrapment efficiency was determined by an ultrafiltration method. Briefly, 1 mL of liposphere dispersion was placed into an Amicon Ultra 4 centrifugal filter unit with a nominal molecular weight cut off 10 kDa (Merck Milipore Ltd., Germany) and centrifuged at 10,000 rpm for 15 min. The free drugs present in filtrate were measured by RP-HPLC (described in Section 2.2.). The amount of drug entrapped was obtained by subtracting the amount of free drug from the total drug incorporated in 1 mL of liposphere dispersion. The

percentage entrapment efficiency (% EE) was calculated using following equation given below.

$$\% \quad EE = \frac{\text{Amount of drug entrapped}}{\text{Total amount of drug taken}} \times 100 \quad (1)$$

2.4. In vitro release

In vitro drug release study was performed by dialysis bag method. Total amount of 300 µg/mL concentration of CBZ TMQ LSP dispersion was placed in preactivated dialysis membrane with a molecular weight cut-off of 12 kDa. Then the closed dialysis pouch were placed in 28 mL of release media (PBS with 0.5% w/v tween 80) containing tubing and placed in shaker bath, with 100 rpm at 37 °C. At predetermined time intervals 2 mL of sample was withdrawn, replaced with fresh medium and analysed for drug content by HPLC method (Section 2.2.1.). Further *in vitro* drug release data obtained was fitted into Zero Order, First Order, Higuchi and Peppas models to study the drug release kinetics from developed formulation. Particle size, PDI and zeta potential were monitored for CBZ TMQ LSP during drug release.

2.5. Cell viability studies

Cell viability was determined using MTT assay (Muntimadugu et al., 2016). MCF-7, MDA-MB-231 cells were plated into 96-well plates at 7×10^3 cells/well using DMEM medium supplemented with 10% FBS. After 24 h, the cells were treated with CBZ solution, TMQ solution and CBZ and TMQ combination solution, CBZ and TMQ co-loaded LSP (0.001–100 µg/mL concentrations) and incubated for 48 h. These cells were treated with 200 µL of MTT solution (500 µg/mL) and incubated for 4 h. After incubation, the cells were treated with 200 µL of DMSO and the absorbance was measured at 570 nm using plate reader (SpectraMax M4 Multimode,USA).

2.6. Combination index (CI) value

From the above MTT results of individual solutions and combinations solutions and combination formulations data representing dose with effect (% cell death) was entered into free trial version of CompuSyn Software (ComboSyn, Inc. NJ, USA.) (Chou and Martin, 2005) to calculate IC50 value and CI values which implies how the selected drugs combination influence the therapeutic efficacy (CI > 1 – Antagonistic, CI = 1- Additive, CI < 1 – Synergistic) at different combination dosing intervals (Dirican et al., 2014; Chou, 2010).

2.7. Cell uptake studies

Cell uptake studies were performed to determine the cell penetration capacity of developed formulation in comparison with solution. Briefly, cells were seeded (10,000 cells/well) in 24 well plates and incubated for 24 h. Cells were treated with FITC, FITC-LSP dispersed in culture medium for 3 h and washed several times with PBS. Cells were fixed and nuclei were stained using 4, 6-diamidino-2-phenylindole (DAPI) solution (Shen et al., 2014). Fluorescent images were captured using confocal laser scanning microscope (Leica TCS SP8 Laser Scanning Spectral Confocal Microscope).

2.8. Acridine orange ethidium bromide (AO/EtBr) staining

MDA-MB-231 cells were plated at a concentration of 1×10^6 cells/ml and treated with different concentrations (1, 2.5 and 5 ng/mL) of combination solutions and formulations for 48 h. 10 µL of fluorescent dyes containing AO and EtBr were added into each well in equal volumes (10 µg/mL) respectively then the cells were visualized immediately under fluorescence microscope (Nikon, Inc. Japan) with excitation (488 nm) and emission (550 nm) at 200x magnification (Kasibhatla et al., 2006).

2.9. DAPI nucleic acid staining

Morphological changes in nucleus were observed through DAPI staining. After treatment with different concentrations (1, 2.5 and 5 ng/mL) of combination solutions and formulations for 48 h, MDA-MB-231 cells were washed with PBS and fixed with 4% formaldehyde then permeabilized with 0.1% Triton X-100 for 10 min followed by staining with 1 µM DAPI. Control and treated cells were observed with fluorescence microscope with excitation at 359 nm and emission at 461 nm using DAPI filter at 200x magnification.

2.10. Cell cycle analysis

MDA-MB-231 cells were seeded in 6 well plates at a density of 1×10^5 cells/mL and incubated for 24 h. Cells were treated with different formulations for 48 h to know the effect on cell cycle. After treatment period, cells were washed with 150 mM PBS, harvested using trypsin EDTA, fixed in 70% chilled ethanol and stored overnight at 2–8 °C. Fixed cells were pelleted, resuspended and treated with RNAse A for 15 min to denature RNA. Then cell nuclei were stained by propidium iodide reagent (400 µg/mL) and incubated for 30 min at 37 °C in dark. Flow cytometric analysis (BD FACSVerse™, USA) was performed by doublet discrimination module with 10,000 events.

2.11. Flow cytometric detection of apoptosis on MDA-MB-231 cells

MDA-MB-231 cells (1×10^6 cells/well) were seeded in 6-well culture plates and allowed to attach for 24 h. Cells were treated with CBZ solution, TMQ solution, CBZ TMQ combination solution, CBZ TMQ LSP for 48 h. After incubation cells were trypsinized and centrifuged at 1000 rpm for 5 min. Extent of apoptosis was determined using the Annexin V-FITC and PI dead cell apoptosis kit (Molecular Probes, Thermo Fisher Scientific, USA) as per manufacturer's protocol and the treated cells were analyzed using flow cytometer (BD FACSVerse™, USA) (Kulhari et al., 2015).

3. Results and discussion

3.1. Preparation and optimization of CBZ TMQ co-loaded LSP

Particle size and EE were considered as important parameters for optimization of LSP which will play crucial role in tumor penetration as well as to get therapeutic efficacy. CBZ TMQ co-loaded LSP were prepared by melt dispersion method. Optimization studies were performed initially for selection of solvent (NMP/ethanol) by keeping other parameters constant like type of core lipid (TC), coat lipid (Egg PC), surfactants (Tween 80, Vitamin E-TPGS) and their ratios (2:1:1:2) w/w respectively. Percentage DL was also kept constant for each drug (1.515) and monitored for particle size and PDI. For CBZ TMQ co-loaded LSP with NMP as solvent resulted in particle size (190.66 ± 1.76 nm), PDI (0.336 ± 0.02) and zeta potential (-32.13 ± 1.078 mV) respectively. Whereas CBZ TMQ co-loaded LSP with ethanol as a solvent gave particle size (116.83 ± 1.05 nm), PDI (0.24 ± 0.008) and zeta potential (-36.6 ± 0.556 mV) respectively which was selected for further studies.

Different core lipids for optimization such as TC, TM, TS, TO and TP were screened with 1.515% DL for each drug (Fig. 1A). These core lipids resulted in particle size 116.83 ± 1.05, 239.2 ± 10.71, 273.46 ± 5.83, 130.1 ± 2.98 and 189.6 ± 7.95 nm with PDI 0.240 ± 0.008, 0.385 ± 0.053, 0.391 ± 0.047, 0.156 ± 0.033 and 0.311 ± 0.037 and zeta potential of -36.6 ± 0.556, -36.4 ± 3.511, -24.13 ± 0.450, -43.86 ± 3.098 and -25.93 ± 0.986 mV (Fig. 1B) respectively. Based on less particle size and PDI with TC and TO as core

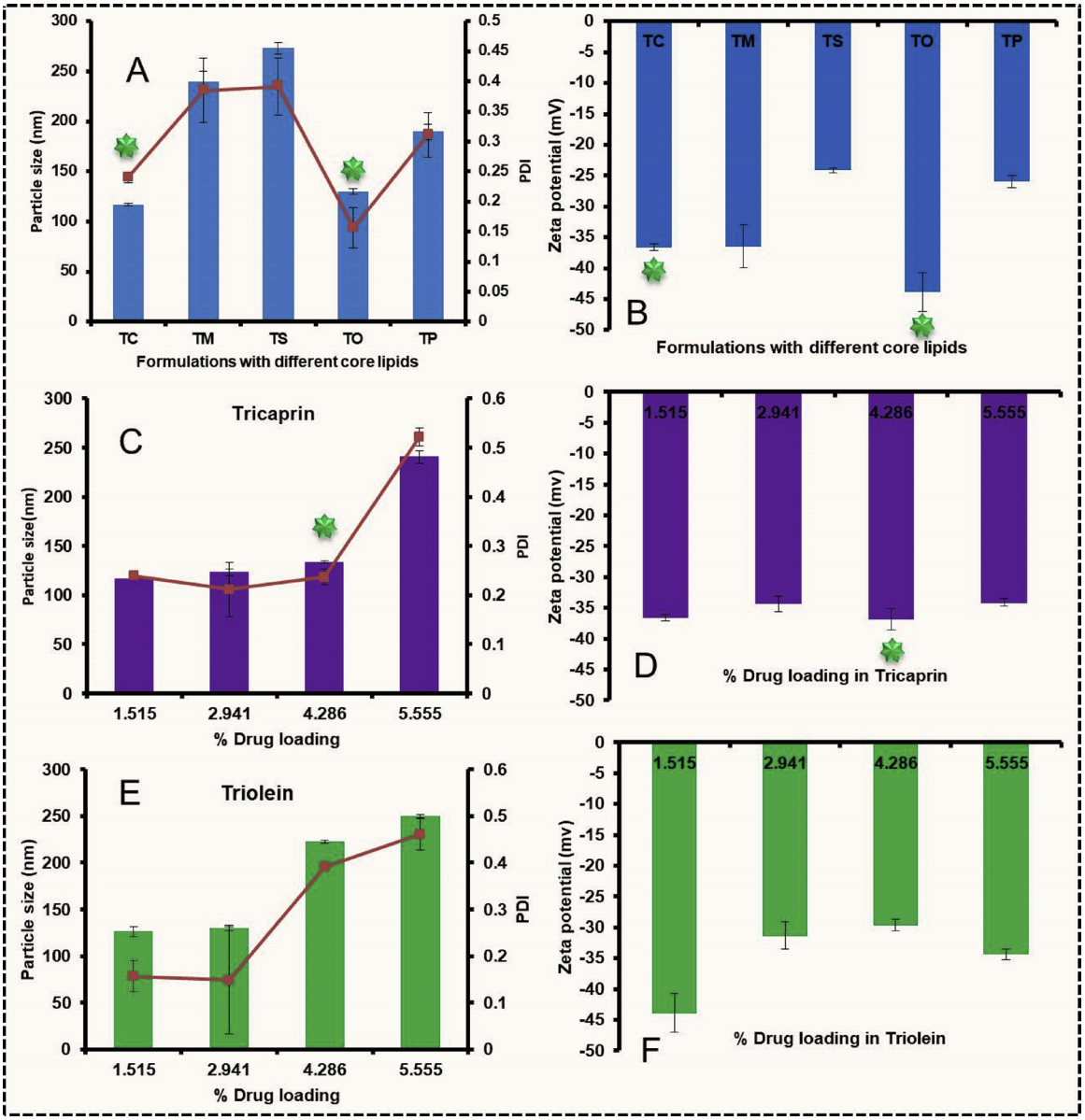

Fig. 1. Preparation and optimization of CBZ and TMQ co-loaded LSP: A and B represents effect of particle size, PDI and zeta potential with different core lipids, C and D represents effect of drug loading on particle size, PDI and zeta potential of LSP with TC as core lipid, E and F represents effect of drug loading on particle size, PDI and zeta potential of LSP with TO as core lipid respectively. The green stars representing final optimized formulation carried out for further studies.

lipids were selected for further studies.

CBZ TMQ co-loaded LSP with % DL for each drug CBZ and TMQ in TC and TO were varied as 1.515, 2.941, 4.286, and 5.555 and evaluated for particle size, PDI, zeta potential. CBZ TMQ co-loaded LSP with TC as core lipid resulted in particle size 116.83 ± 1.05, 123.5 ± 3.15, 133.56 ± 1.33 and 240.4 ± 5.89 nm with PDI 0.240 ± 0.008, 0.211 ± 0.055, 0.237 ± 0.016 and 0.522 ± 0.018 (Fig. 1C) and zeta potential of -36.6 ± 0.556, -34.36 ± 1.23, -36.83 ± 1.720 and -34.16 ± 0.602 mV (Fig. 1D) respectively. CBZ TMQ co-loaded LSP with TO as core lipid resulted in particle size 126.23 ± 5.04, 130.1 ± 2.98, 222.8 ± 1.83 and 249.96 ± 1.77 nm with PDI 0.156 ± 0.033, 0.114 ± 0.031, 0.391 ± 0.008 and 0.461 ± 0.033 (Fig. 1E) and zeta potential of -43.86 ± 3.098, -31.33 ± 2.20, -29.63 ± 0.923 and -34.36 ± 0.923 mV (Fig. 1**F**) respectively.

From the above results CBZ TMQ co-loaded LSP with TC as core lipid with 4.286% DL for CBZ and TMQ with less particle size and PDI was with % EE of 90.80 ± 0.022 of TMQ and 98.92 ± 0.12 for CBZ was selected for further studies. Particle size and zeta potential, SEM and TEM images for optimized CBZ TMQ co-loaded LSP were shown in Fig. 2**A, 2B, 2C** and **2D** respectively.

3.2. *In vitro* drug release

The % cumulative drug release for TMQ from CBZ TMQ co-loaded LSP in PBS with 0.5% w/v tween 80 was found to be 51.58 ± 0.158 in 2 h. *In vitro* drug release profile (**Fig. 3A**) for CBZ from CBZ TMQ co-loaded LSP PBS with 0.5% w/v tween 80, % cumulative drug release was found to be 97.98 ± 3.28 respectively in 96 h and evaluated for drug release kinetics (Zero Order, First Order, Higuchi and Peppas as shown in Fig. 3B**, 3C, 3D and 3E** respectively.) to understand the drug release mechanism from liposphere system. Higuchi release pattern was observed with CBZ TMQ LSP with R^2 value of 0.9901. The release mechanism was determined as anomalous non-fickian diffusion based on the "n" value (0.5672) calculated using Peppas equation. Particle size, PDI and zeta potential before drug release were found to be 131.8 ± 1.3 nm, 0.229 ± 0.01 and -26.43 ± 0.057 mV respectively.

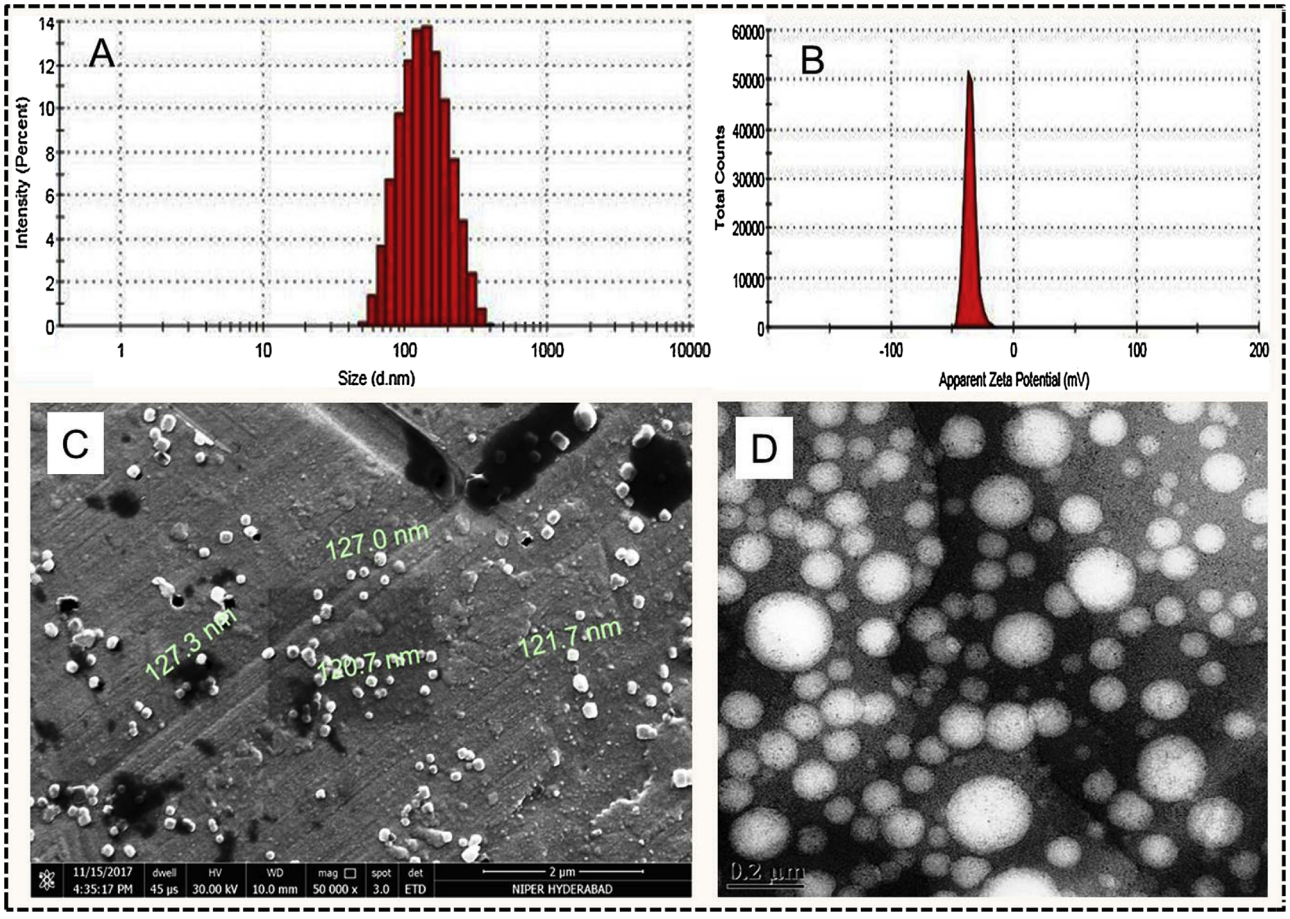

Fig. 2. Characterization of CBZ and TMQ co-loaded LSP: A and B represent particle size distribution and zeta potential graphs from zeta analyser. C and D represents SEM and TEM images of CBZ and TMQ co-loaded LSP respectively.

Increase in particle size between 2–6 h of release time point due to swelling of matrix then slow reduction in particle size was due to erosion of matrix from LSP. After 96 h drug release from dialysis particle size, PDI and zeta potential were found to be 111.06 ± 1.09 nm, 0.34 and – 4.2 mV respectively, drastic changes in particle size, PDI and zeta potential were observed as shown in Figs. 3**F, G and H**. Reduction in particle size and increase in zeta potential is due to diffusion and erosion based release of drugs from CZB TMQ co-loaded LSP.

3.3. Cell viability studies with combination index value

Dose dependent reduction in % cell viability was observed on MCF-7 and MDA-MB-231 cell lines up on treatment with CBZ solution, TMQ solution, CBZ TMQ solution, CBZ TMQ LSP at a concentration of 1 ng/mL to 100 µg/ mL (Fig. 4**A and B**). Dose with effect values were kept in CompuSyn software for all treatment groups to get IC50 value as well as combination index values. IC50 values in MCF-7 cells for CBZ solution, TMQ solution, CBZ TMQ solution, CBZ TMQ LSP were found to be 34.27 ng/mL, 2.74 µg/mL, 13.57 ng/mL and 10.42 ng/mL respectively. However, combination solution has shown 2.5, 202 fold reduction in IC50 value in comparison to CBZ solution and TMQ solution respectively. IC50 values in MDA-MB-231 cells for CBZ solution, TMQ solution, CBZ TMQ solution, CBZ TMQ LSP were found to be 29.64 ng/mL, 9.15 µg/mL, 14.39 ng/mL and 7.63 ng/mL. Above IC50 values indicating that combination solution has shown 2, 636 fold reduction in IC50 value in comparison to CBZ solution and TMQ solution respectively. From the above results it was observed that combination is more effective. More over CBZ TMQ LSP has shown 1.3, 1.9 fold reduction in IC50 value in MCF-7 and MDA-MB-231cells respectively, which was proven by CI values at different doses of CBZ TMQ solution (0.288, 0.15, 0.117, 0.254, 0.46, and 0.175) and CBZ TMQ LSP (0.18, 0.12, 0.117, 0.11, 0.086 and 0.041) in MCF-7 cell lines. At all doses CI values < 1 indicated strong synergistic combination (Fig. 4**A'**). Similarly, in MDA-MB-231 cell lines CI values at different doses of CBZ TMQ solution (0.218, 0.269, 0.201, 0.11, 0.12, and 0.02) and CBZ TMQ LSP (0.054, 0.106, 0.201, 0.146, 0.081 and 0.007) were observed below 1(Fig. 4**B'**) implicated synergistic activity for breast cancer. As increase in dose there was an increase in Fa value in CI plot due to increase in cell death was observed (Fig.4**A' and B'**) which was more prominent in CBZ TMQ LSP may be due to rapid cellular internalization.

3.4. Cell uptake studies

Uptake efficiency of FITC solution and FITC loaded LSP were qualitatively visualized by confocal laser scanning microscopy as shown in Fig. 5. There was less intensity of green fluorescence observed with the cells treated with FITC solution as it is highly hydrophobic and cannot permeate through the cell membranes. Whereas, the cells treated with FITC loaded LSP had shown an increase in green fluorescence intensity which implies the more cell permeability in cancer cells. Increase in cellular internalization is due to lipid based components of LSP with nano size range which will be more beneficial for cancer treatment.

3.5. Acridine orange ethidium bromide (AO/EtBr) staining

The effect of CBZ TMQ solution and CBZ TMQ LSP at different concentrations (1, 2.5, 5 ng/mL) on cellular morphology on MDA-MB-231 cell lines were analysed by AO/EtBr staining technique as shown in

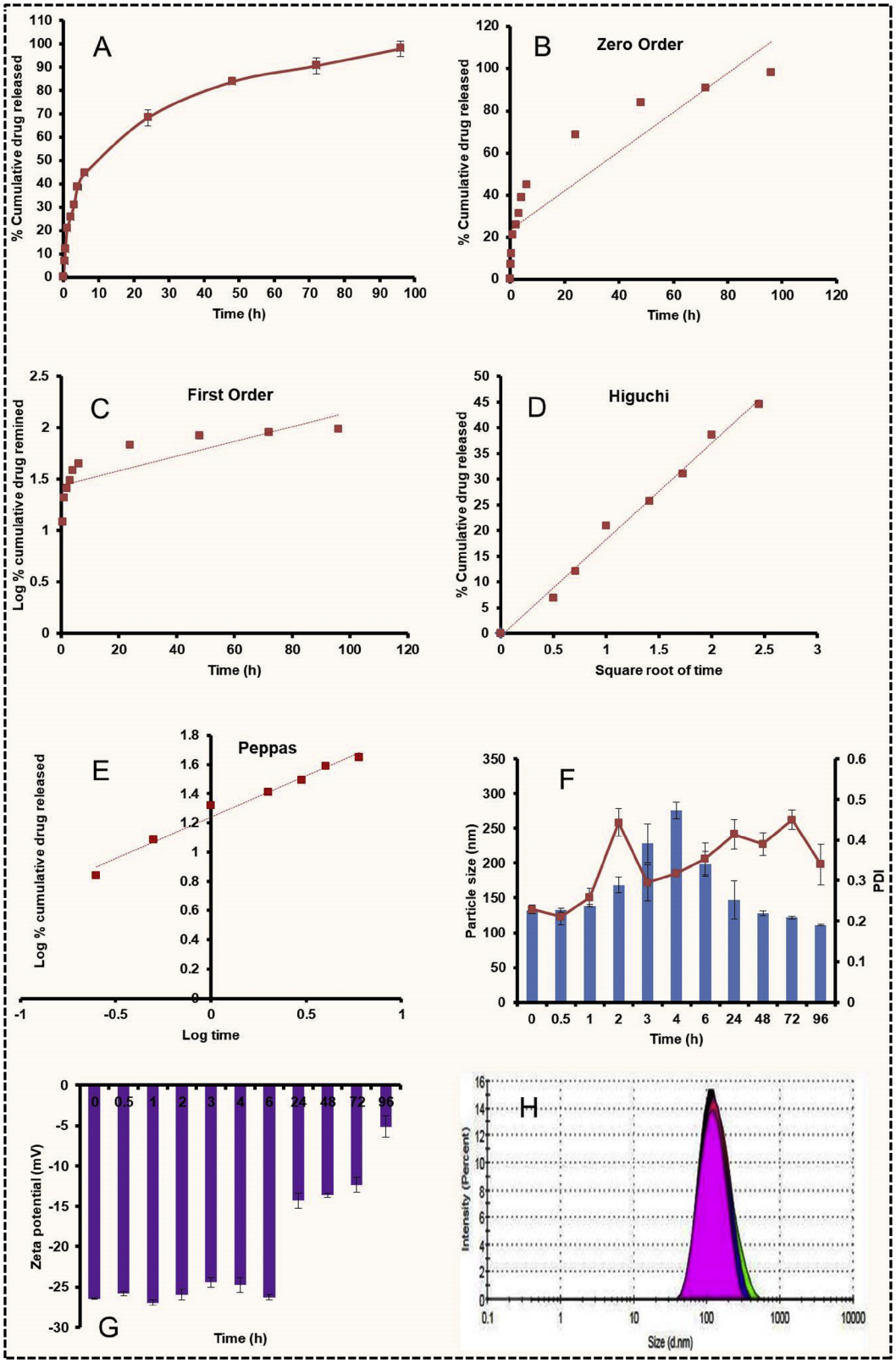

Fig. 3. *In vitro* drug release from LSP: A represents % cumulative drug release vs time plot for CBZ from LSP, B, C, D and E represents drug release kinetics models (Zero Order, First Order, Higuchi and Peppas respectively). F and G represent average particle size and zeta potential at different release time points. H represent overlay of particle size distribution plot before and after dialysis by dynamic light scattering technique.

Fig. 6. The staining reagent is used for easy differentiation between live, apoptotic and dead cells. The single staining solution is a mixture of AO for live cell identification and EtBr for identification of dead cells. The AO stained live cells appear green and EtBr stained dead cells appear red when visualized by fluorescent microscopy. In control appearance of viable cells with intact green nucleus was observed. When cells were treated with the CBZ TMQ solution and CBZ TMQ LSP morphological changes are observed like bright-green nucleus showing condensation

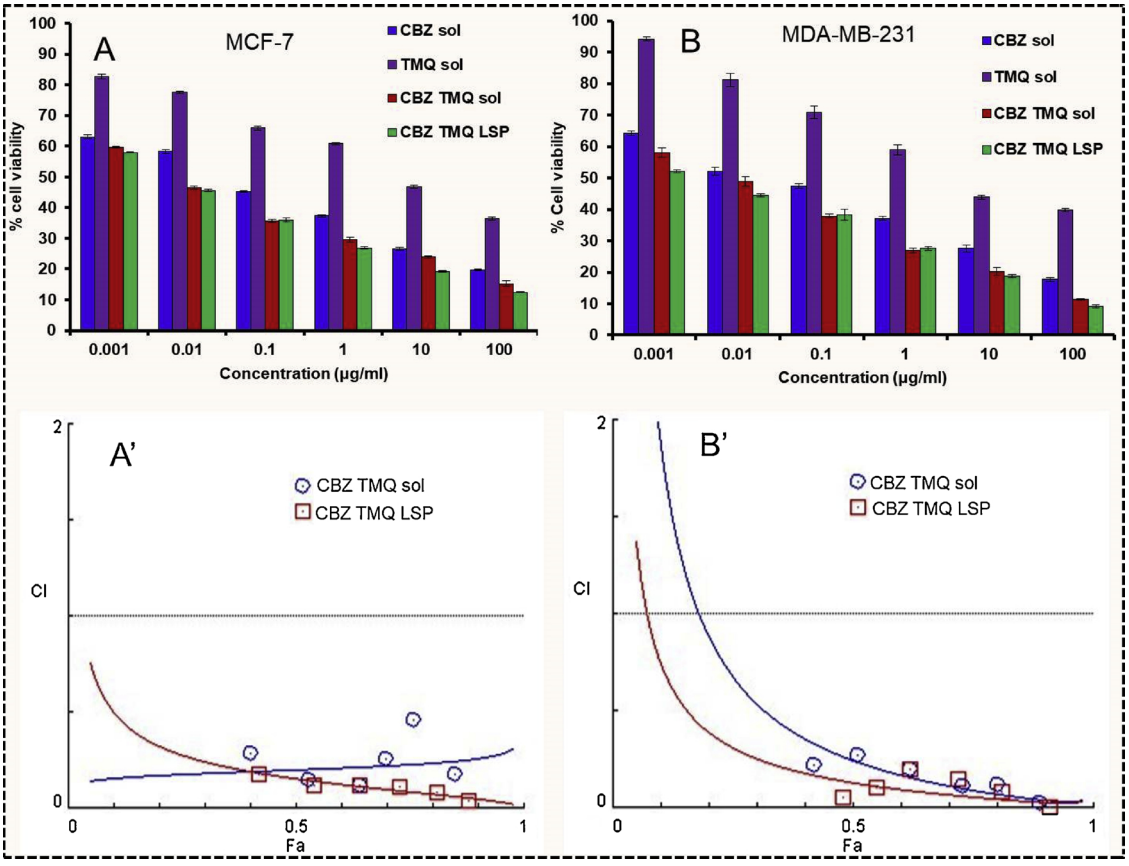

Fig. 4. Cell viability studies with Combination Index Plots: A and B represents % cell viability graph of MCF-7, MDA-MB-231 cells upon treatment with different concentrations of CBZ sol, TMQ sol, CBZ TMQ sol and CBZ TMQ LSP, as increase in concentration there was a drastic reduction in % cell viability was observed. A' and B' represents combination index plots of MCF-7, MDA-MB-231 cells upon treatment with different concentrations of CBZ TMQ sol and CBZ TMQ LSP respectively. In both the plots CI values for selected doses were found to be less than 1 implies selected drug combination is showing strong synergism.

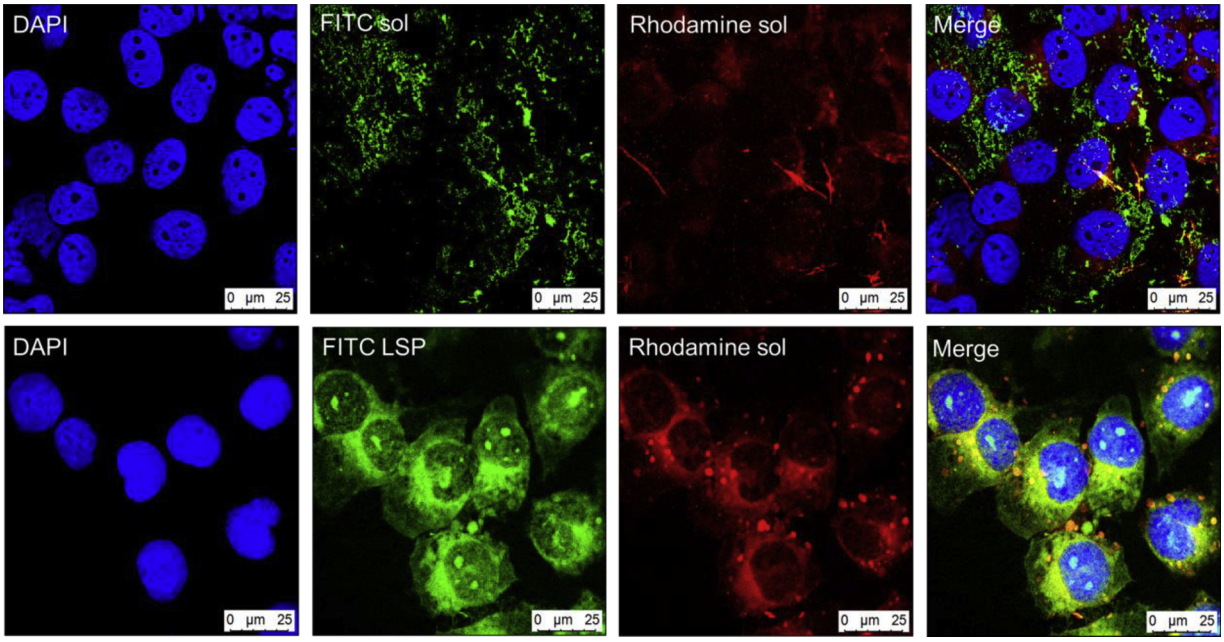

Fig. 5. Cell uptake studies: Uptake efficiency of FITC sol and FITC loaded LSP on MDA-MB-231 cells by confocal laser scanning microscopic imaging. First row represents cells treated with DAPI, FITC sol, Rhodamine sol and merge image. Second row is cells treated with DAPI, FITC loaded LSP, Rhodamine sol and merge image respectively. FITC loaded LSP have shown more intense fluorescence when compared to FITC sol. So, LSP have more cellular internalization which was proved by confocal imaging.

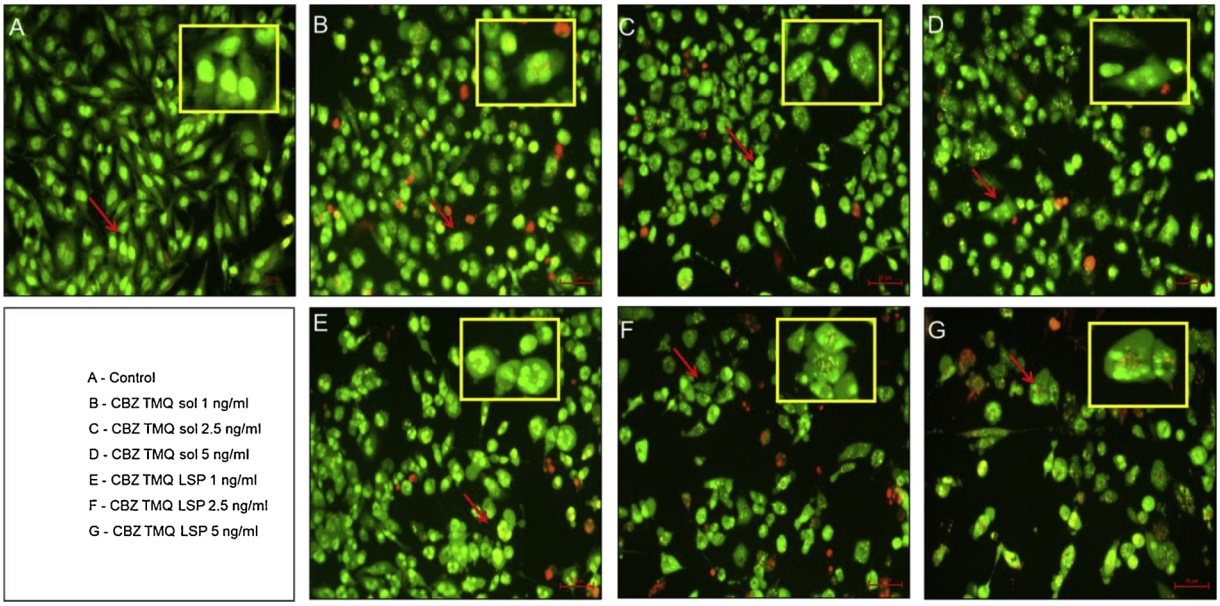

Fig. 6. Acridine orange ethidium bromide (AO/EtBr) staining on MDA-MB-231 cells: A represents normal control without treatment stained with AO implies cells are healthy and live, B, C and D represents cells treated with CBZ and TMQ combination solution at concentrations of 1, 2.5 and 5 ng/mL respectively and stained with AO/EtBr, E, F and G represents cells treated with CBZ and TMQ co-loaded LSP at concentrations of 1, 2.5 and 5 ng/mL respectively and stained with AO/EtBr. As increase in treatment dose abnormal changes in cell morphology with cell membrane blebbing, DNA fragmentation, cell death was observed along with decrease in cell density which is hall marks of apoptosis.

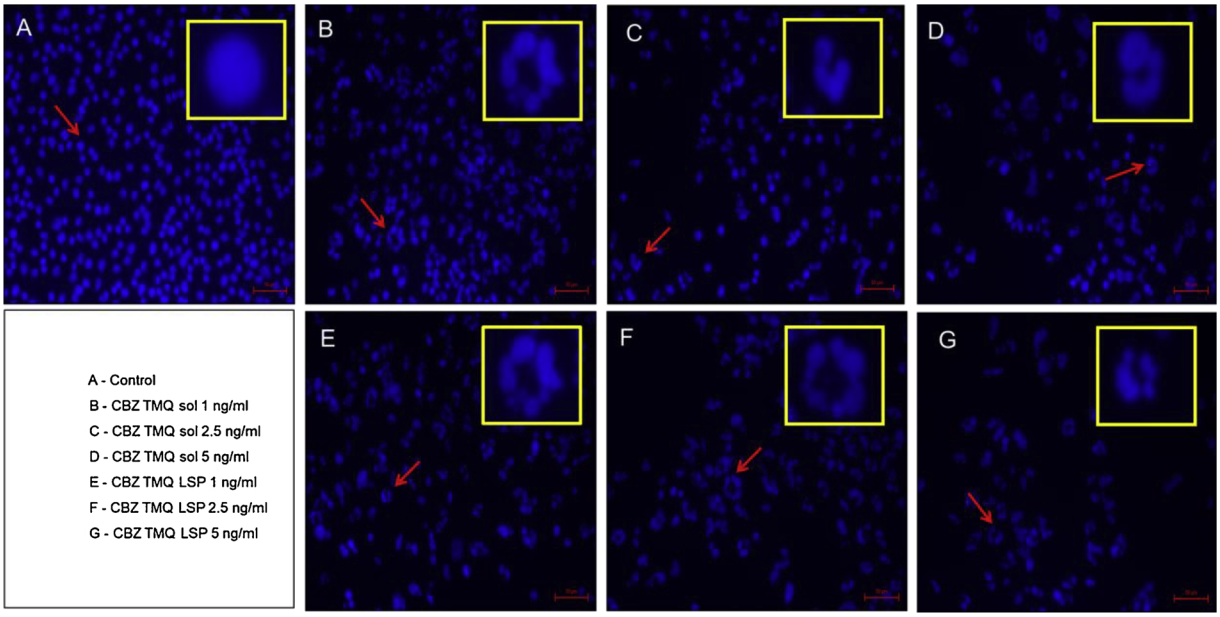

Fig. 7. DAPI nucleic acid staining on MDA-MB-231 cells: A represents normal control without treatment stained with DAPI, B, C and D represents cells treated with CBZ and TMQ combination solution at concentrations of 1, 2.5 and 5 ng/ mL respectively and stained with DAPI, E, F and G represents cells treated with CBZ and TMQ co-loaded LSP at concentrations of 1, 2.5 and 5 ng/ mL respectively and stained with DAPI. As increase in treatment dose there was a drastic changes in nuclear morphology was observed with nuclear fragmentation and condensation with horse shoe shaped nucleus as well as decrease in nuclear density was observed.

and fragmentation of chromatin in the nucleus with cell shrinkage, dense orange areas of chromatin condensation, membrane blebbing and red colour cells implicated cellular death. As increase in concentration there were drastic changes in cellular morphology and decrease in cell density was observed with the cells treated with CBZ TMQ solution which was more prominently observed in cells treated with CBZ TMQ LSP. These results explore that CBZ TMQ solution and CBZ TMQ LSP may induce apoptosis as evident by observed hall marks of apoptosis.

3.6. DAPI nucleic acid staining

Nuclear morphology of MDA-MB-231 cells treated with CBZ TMQ solution and CBZ TMQ LSP at different concentrations (1, 2.5, 5 ng/mL) were determined by using DAPI staining method. The blue-fluorescent DAPI is a nuclear counter stain preferentially stains dsDNA. DAPI or 4′, 6-diamidino-2-phenylindole is a fluorescent stain that binds strongly to A–T rich regions in DNA. Upon treatment with CBZ TMQ solution and

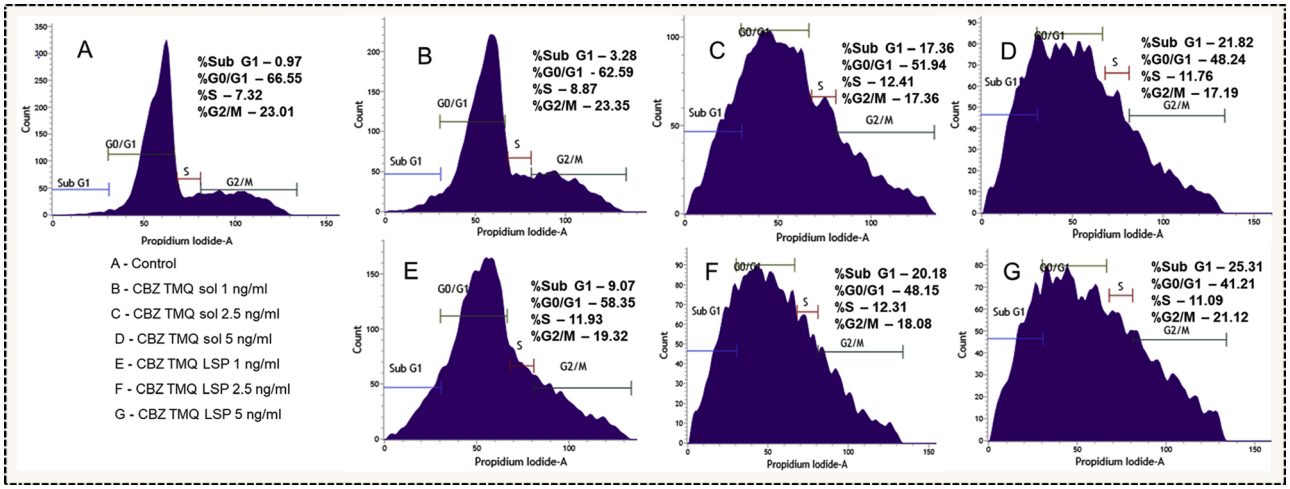

Fig. 8. Cell cycle analysis: on MDA-MB-231 cells, A. flow cytogram of vehicle control without treatment, B, C and D represents flowcytograms of cells treated with CBZ and TMQ combination solution at concentrations of 1, 2.5 and 5 ng/mL respectively, E, F and G represents apoptotic flowcytograms of cells treated with CBZ and TMQ co-loaded LSP at concentrations of 1, 2.5 and 5 ng/mL respectively. As increase in dose there was an increase in sub G1 population was observed in both the groups. But the results were more prominent in CBZ and TMQ co-loaded LSP group.

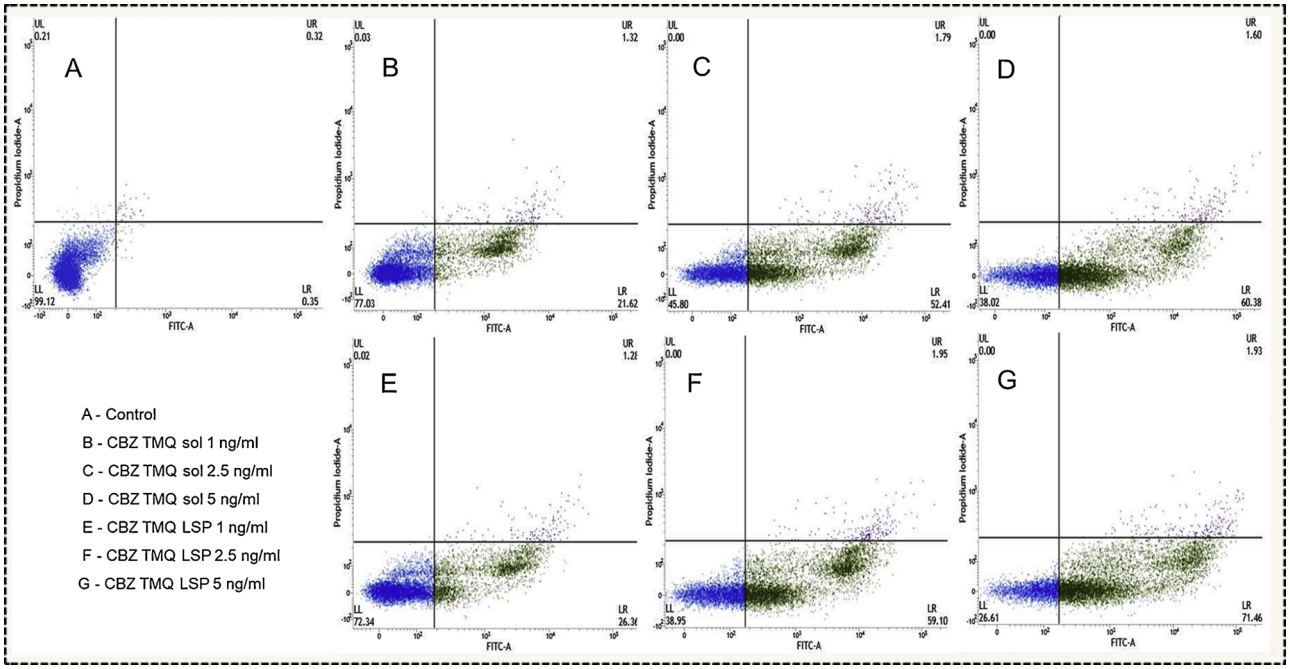

Fig. 9. Flow cytometric detection of Apoptosis on MDA-MB-231 Cells: Lower Left (LL) quadrant represents live cells, Lower Right (LR) quadrant represents cells which are in early apoptotic phase, Upper Right (UR) quadrant represents cells which are in late apoptotic phase, Upper Left quadrant represents cells which are in necrotic phase (Dead). A. Control cells without treatment, B, C and D represents apoptotic flowcytograms of cells treated with CBZ and TMQ combination solution at concentrations of 1, 2.5 and 5 ng/mL respectively, E, F and G represents apoptotic flowcytograms of cells treated with CBZ and TMQ co-loaded LSP at concentrations of 1, 2.5 and 5 ng/mL respectively. As increase in dose there was a drastic increase in early apoptosis was observed in both the groups but which was more prominently observed in CBZ and TMQ co-loaded LSP.

CBZ TMQ LSP at different concentration remarkable changes in nucleus was observed when compared to vehicle control. As increase in concentration of CBZ TMQ solution and CBZ TMQ LSP horse shoe nucleus along with DNA fragmentation is observed with decrease in nuclear density was observed as shown in Fig. 7. DAPI staining explained that treated cells with CBZ TMQ solution are inducing significant nuclear morphological changes which are more prominently observed in cells treated with CBZ TMQ LSP are hall marks of apoptosis.

3.7. Cell cycle analysis

Flow cytometry analysis was performed after treating MDA-MB-231 cells with CBZ TMQ solution and CBZ TMQ LSP at different concentrations (1, 2.5, 5 ng/mL) to study the distribution of cells in different phases (sub G1 *vs.* G0/G1 *vs.* S *vs.* G2/M) and also to detect apoptotic cells with fractional DNA content. As increase in concentration of treatment groups there was a drastic reduction in G0/G1 phase arrest and increase in sub G1 populations were observed in comparison to control. Upon treatment with CBZ TMQ solution at 1, 2.5 and 5 ng/mL. Percentage sub G1 population (3.28, 17.36 and 21.82 respectively) was increased in concentration dependent manner which implicates that the cells are undergoing apoptosis. Whereas, with CBZ TMQ LSP at 1, 2.5 and 5 ng/mL percentage sub G1 population (9.07, 20.18 and 25.31 respectively) was more as shown in Fig. 8. CBZ TMQ LSP have

shown 2.8, 1.2 and 1.2 fold increase in sub G1 population in comparison to CBZ TMQ sol at 1, 2.5 and 5 ng/mL concentration respectively.

3.8. Flow cytometric detection of apoptosis on MDA-MB-231 cells

Quantitative determination of induction of apoptosis in MDA-MB-231 cell lines upon treatment with CBZ TMQ solution and CBZ TMQ LSP was studied by flow cytometric analysis which was compared with vehicle control. Upon treatment there was a dose dependent increase in percentage of early phase apoptotic cells was observed with CBZ TMQ solution at 1, 2.5 and 5 ng/ mL (21.62, 52.41 and 60.38 respectively). Whereas, the cells treated with CBZ TMQ LSP at 1, 2.5 and 5 ng/ mL concentration had shown more prominent increase in percentage of early phase apoptotic cells (26.36, 59.10 and 71.46 respectively) as shown in Fig. 9. CBZ TMQ LSP have shown 1.2, 1.1 and 1.2 fold increase in early apoptotic cells in comparison to CBZ TMQ sol at 1, 2.5 and 5 ng/mL concentration respectively.

4. Conclusion

Co-delivery of synergistic drug combination from a single carrier system like LSP offers simultaneous delivery which will aid better therapeutic activity. Co-loaded LSP were developed for highly hydrophobic and unstable drugs like CBZ and TMQ with a particle size less than 150 nm which is more beneficial for passive targeting in tumors by EPR effect. CBZ and TMQ loading (for each drug with 4.268% w/w) were optimized with an entrapment efficiency of more than 90% for both the drugs. *In vitro* drug release studies revealed more than 50% of TMQ was released in 2 h and more than 95% of CBZ was released from CBZ TMQ LSP in 96 h. From the release kinetics it was observe that CBZ TMQ LSP system followed Higuchi model with anomalous non-fickian diffusion which is beneficial for sustained tumor therapy for prolonged period of time. Cell culture experiments proved that CBZ and TMQ acting as a synergistic combination to enhance the cell death by apoptosis due to rapid cellular internalization of LSP which was observed in cancer cells by confocal microscopic imaging. Other advantage of this combination that is CBZ is P-gp substrate whereas TMQ act as P-gp inhibitor which may enhance the efficacy in treatment of breast cancer. Developed CBZ TMQ co-loaded LSP are scalable and industrially feasible with enhanced clinical benefit in breast cancer cell lines. Further in depth studies are required to prove the anti-tumor efficacy.

Conflict of interest

The authors have no relevant affiliations or financial involvement with any organization or entity with a financial interest in or financial conflict with the subject matter or materials discussed in the manuscript. This includes employment, consultancies, honoraria, stock ownership or options, expert testimony, grants or patents received or pending, or royalties.

Acknowledgement

Authors are thankful to NIPER-Hyderabad for providing required facilities, support and encouragement throughout the project. Authors thank Department of Biotechnology, Government of India (Grant no: 6242-P41/RGCB/PMD/DBT/WHDK/2015) for providing Cell culture facility. Authors are also grateful to TherDose Pharma Pvt. Ltd. for providing cabazitaxel and for research purpose.

References

Al-Lazikani, B., Banerji, U., Workman, P., 2012. Combinatorial drug therapy for cancer in the post-genomic era. Nat. Biotechnol. 30 (7), 679.
Avramoff, A., et al., 2012. Cyclosporin pro-dispersion liposphere formulation. J. Control. Release 160 (2), 401–406.
Bekerman, T., Golenser, J., Domb, A., 2004. Cyclosporin nanoparticulate lipospheres for oral administration. J. Pharm. Sci. 93 (5), 1264–1270.
Chou, T.-C., 2010. Drug combination studies and their synergy quantification using the Chou-Talalay method. Cancer Res. 70 (2), 440–446.
Chou, T., Martin, N., 2005. Compusyn For Drug Combinations: PC Software and User's Guide: a Computer Program for Quantitation of Synergism and Antagonism in Drug Combinations, and the Determination of IC50 and ED50 and LD50 Values. ComboSyn Inc, Paramus,(NJ).
Dirican, A., et al., 2014. Enhanced cytotoxicity and apoptosis by thymoquinone in combination with zoledronic acid in hormone-and drug-resistant prostate cancer cell lines. J. BUON 19 (4), 1055–1061.
Elgart, A., et al., 2012. Lipospheres and pro-nano lipospheres for delivery of poorly water soluble compounds. Chem. Phys. Lipids 165 (4), 438–453.
Gali-Muhtasib, H., Roessner, A., Schneider-Stock, R., 2006. Thymoquinone: a promising anti-cancer drug from natural sources. Int. J. Biochem. Cell Biol. 38 (8), 1249–1253.
Jain, A., et al., 2016. Tacrolimus and curcumin co-loaded liposphere gel: synergistic combination towards management of psoriasis. J. Control. Release 243, 132–145.
Jain, A., et al., 2017. Liposphere mediated topical delivery of thymoquinone in the treatment of psoriasis. Nanomed. Nanotechnol. Biol. Med. 13 (7), 2251–2262.
Jordan, M.A., Wilson, L., 2004. Microtubules as a target for anticancer drugs. Nat. Rev. Cancer 4 (4), 253.
Kasibhatla, S., et al., 2006. Acridine orange/ethidium bromide (AO/EB) staining to detect apoptosis. Cold Spring Harb. Protoc. 2006 (3) p. pdb. prot4493.
Khan, M.A., et al., 2017. Thymoquinone, as an anticancer molecule: from basic research to clinical investigation. Oncotarget 8 (31), 51907.
Kitano, H., 2004. Cancer as a robust system: implications for anticancer therapy. Nat. Rev. Cancer 4 (3), 227.
Kodappully Sivaraman Siveen, N.M., et al., 2014. Thymoquinone overcomes chemoresistance and enhances the anticancer effects of bortezomib through abrogation of NF-κB regulated gene products in multiple myeloma xenograft mouse model. Oncotarget 5 (3), 634.
Kulhari, H., et al., 2015. Cyclic-RGDfK peptide conjugated succinoyl-TPGS nanomicelles for targeted delivery of docetaxel to integrin receptor over-expressing angiogenic tumours. Nanomed. Nanotechnol. Biol. Med. 11 (6), 1511–1520.
Kümmel, S., et al., 2017. Randomised, open-label, phase II study comparing the efficacy and the safety of cabazitaxel versus weekly paclitaxel given as neoadjuvant treatment in patients with operable triple-negative or luminal B/HER2-negative breast cancer (GENEVIEVE). Eur. J. Cancer 84, 1–8.
Lebwohl, M., Ali, S., 2001. Treatment of psoriasis. Part 1. Topical therapy and phototherapy. J. Am. Acad. Dermatol. 45 (4), 487–502.
Lydon, A., 2011. Cabazitaxel side effects: prevention and management. Br. J. Med. Surg. Urol. 4, S21–S27.
Ma, L., Kohli, M., Smith, A., 2013. Nanoparticles for combination drug therapy. ACS Nano 7 (11), 9518–9525.
Mahajan, M., et al., 2015. Emerging strategies and challenges for controlled delivery of taxanes: a comprehensive review. Curr. Drug Metab. 16 (6), 453–473.
Miller, K.D., et al., 2016. Cancer treatment and survivorship statistics, 2016. CA Cancer J. Clin. 66 (4), 271–289.
Mostofa, A., et al., 2017. Thymoquinone as a potential adjuvant therapy for Cancer treatment: evidence from preclinical studies. Front. Pharmacol. 8, 295.
Muntimadugu, E., et al., 2016. CD44 targeted chemotherapy for co-eradication of breast cancer stem cells and cancer cells using polymeric nanoparticles of salinomycin and paclitaxel. Colloids Surf. B: Biointerfaces 143, 532–546.
Muntimadugu, E., Kommineni, N., Khan, W., 2017. Exploring the potential of nanotherapeutics in targeting tumor microenvironment for cancer therapy. Pharmacol. Res. 126, 109–122.
Peer, D., et al., 2007. Nanocarriers as an emerging platform for cancer therapy. Nat. Nanotechnol. 2 (12), 751.
Pratama, M.R.F., 2017. Habbatus Sauda (Nigella Sativa) Sebagai Antikanker Paudara: Bukan Sekedar Timokuinon (Habbatus Sauda (Nigella Sativa) As Anti-breast Cancer: Not Only Thymoquinone).
Pratt, W.B., Ensminger, W.D., Ruddon, R.W., 1994. The Anticancer Drugs. Oxford University Press, USA.
Rahmani, A.H., et al., 2014. Therapeutic implications of black seed and its constituent thymoquinone in the prevention of cancer through inactivation and activation of molecular pathways. Evid. Based Complement. Altern. Med. 2014.
Reddy, L.H., Bazile, D., 2014. Drug delivery design for intravenous route with integrated physicochemistry, pharmacokinetics and pharmacodynamics: illustration with the case of taxane therapeutics. Adv. Drug Deliv. Rev. 71, 34–57.
Salmani, J.M.M., et al., 2014. Aqueous solubility and degradation kinetics of the phytochemical anticancer thymoquinone; probing the effects of solvents, pH and light. Molecules 19 (5), 5925–5939.
Shen, J., et al., 2014. Cyclodextrin and polyethylenimine functionalized mesoporous silica nanoparticles for delivery of siRNA cancer therapeutics. Theranostics 4 (5), 487.
Stewart, B., Wild, C.P., 2017. World Cancer Report 2014. Health.